

Egyptian Apricot Stone (*Prunus armeniaca*) as a Low Cost and Eco-friendly Biosorbent for Oxamyl Removal from Aqueous Solutions

Sahar M. Ahmed¹ and Somaia G. Mohammad^{2*}

¹*Egyptian Petroleum Research Institute, Nasr City, Cairo, Egypt.*

²*Pesticide Residues and Environmental Pollution Department, Agriculture Research Center, Dokki, Giza, Egypt.*

Authors' contributions

This work was carried out in collaboration between all authors. Author SMA managed the analyses of the study and interpretation of data, author SGM designed the study, wrote the protocol and wrote the first draft of the manuscript. All authors read and approved the final manuscript.

Original Research Article

Received 25th September 2013
Accepted 13th November 2013
Published 13th December 2013

ABSTRACT

In this work, activated carbon was prepared from apricot stone (ASAC) waste to remove the insecticide oxamyl from aqueous solutions. The effect of different parameters such as adsorbent dose, the initial oxamyl concentration and contact time were investigated. Adsorption isotherm, kinetics and thermodynamics of oxamyl on ASAC were studied. Equilibrium data were fitted to the Langmuir, Freundlich, Temkin and Dubinin-Radushkevich (D-R) isotherm models. Langmuir isotherm provided the best fit to the equilibrium data with maximum adsorption capacity of 147.05 (mg/g). Kinetic studies were also undertaken in terms of pseudo-first-order, pseudo-second-order and intraparticle diffusion kinetic models for oxamyl on ASAC. The adsorption process follows the pseudo-second order kinetic with high coefficients correlation. The thermodynamic parameters ΔG° , ΔH° and ΔS° determined, showed that the adsorption of oxamyl onto ASAC was feasible, spontaneous and endothermic. The results showed that ASAC is an efficient adsorbent for the adsorptive removal of oxamyl from aqueous solutions.

*Corresponding author: Email: somaigaber@yahoo.com;

Keywords: Oxamyl; apricot stone; activated carbon; adsorption isotherm; kinetics; thermodynamics.

1. INTRODUCTION

Oxamyl, (N,N-dimethylcarbamoxyloxyimino -2- (methylthio) acetamide) is a carbamate compound used in a wide range of agricultural situations. It is systemic and active as an insecticide [1] or a nematicide [2,3]. Oxamyl has high solubility in water (280 g /L) and has a very low soil sorption coefficient. It is used for the control of nematodes in vegetables, bananas, pineapple, peanut, cotton, Soya beans, tobacco, potatoes, sugar beet and other crops. The toxicity of pesticides and their degradation products is making these chemical substances a potential hazard by contaminating our environment [4]. Therefore, the removal of pesticides from water is one of the major environmental concerns these days.

There are several procedures available for pesticides removal from water which includes photocatalytic degradation [5,6], ultrasound combined with photo-Fenton treatment [7], advanced oxidation processes [8], aerobic degradation [9], electro dialysis membranes [10], ozonation [11] and adsorption [12]. ACs has high porosity and therefore has very high surface area for adsorption. In addition, the chemical nature of their surfaces enhances adsorption. Adsorption by activated carbon (AC) is one of the most widely used techniques and has proven to be effective in the removal of pesticides, dyes [13-15] and phenols [16] from aqueous solutions. However, only a limited number of published studies can be found on the use of adsorbent for pesticides removal.

Natural materials that are available in large quantities or certain waste from agricultural operations may have potential to be used as low cost adsorbents, as they represent unused resources, widely available and are environmentally friendly [17].

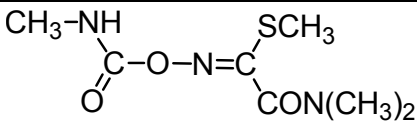
Researchers have investigated the production of AC from many agricultural wastes including pistachio shell, rambutan peel, mangosteen peel, corncob, olive-waste cakes and walnut shells [18-22]. The apricot (*Prunus armeniaca*) is a common fruit in Egypt. The stone fruit cultivated area in Egypt is 49204 ha with an approximate yearly production of 476849 tones (6 % of total fruit production) [23]. Apricot stone as a by-product of the apricot Juice industry is therefore an inexpensive materials. The use of apricot stone as a precursor for activated carbon will provide solution to environmental problems caused by this waste as well as produce a value added product from a low cost material. Therefore, in this study, removal of oxamyl from aqueous solutions on activated carbon prepared from apricot stones (AS) by chemical activation was studied. Experimental parameters affecting the adsorption process such as adsorbent dose, initial oxamyl concentration and contact time for oxamyl removal were optimized. The equilibrium, kinetic and thermodynamic data of the adsorption was studied to describe the adsorption process.

2. MATERIALS AND METHODS

2.1 Adsorbate

The pesticide used as adsorbate in the experiments is oxamyl. Some properties and chemical structure of the pesticide is given in Table 1.

Table 1. Some properties and chemical structure of oxamyl

Common name	Oxamyl
Chemical structure	
Name	N,N-dimethyl-2-methylcarbamoyloxyimino-2- (methylthio) acetamide
Pesticide group	Carbamate
Activity	Systemic insecticide and nematicide
Molecular formula	C7H13N3O3S
MWa	219.3
Sb (g /L)	280 g/L
Formulation	10 % GR
Rate of application	20 Kg/ Feddan

Data were obtained from [24]

- a Molecular weight.
- b Solubility in water at 25°C.

2.2 Adsorbent (ASAC)

Apricot stone was collected from a local market in Egypt.

2.3 Preparation of Activated Carbon

Apricot stone used in this study as precursor was sourced locally. These were washed severally with distilled water to remove water-soluble impurities and dried to constant weight in an oven at 70°C for 2 days. The dried samples were ground and sieved by AS 200 Analytical Sieve Shakers, Retsch GmbH, Germany to particle size of 63 µm and further dried in the oven. The sample was then soaked in orthophosphoric acid (H₃PO₄) with an impregnation ratio of 1:1 (w/w) for 24 h and dehydrated in an oven overnight at 105°C. The resultant sample was activated in a closed muffle furnace to increase the surface area at 500°C for 2 h. The AC produced was cooled to room temperature and washed with 0.1 M HCl and successively with distilled water. Washing with distilled water was done repeatedly until the pH of the filtrate reached 6–7. The final product was dried in an oven at 105°C for 24 h and stored in a vacuum desiccator until needed [25].

2.4 Characterization of Activated Carbon

2.4.1 Scanning electron microscopy and fourier transform infrared study

Scanning electron microscopy (SEM) (JEOL 5400, Japan) analysis was carried out on ASAC to study its surface texture at 30 KV accelerated voltage. Prior to scanning, the adsorbent was coated with a thin layer of gold using a sputter coater to make it conductive. The surface functional groups of ASAC were determined using Fourier transform infrared spectroscopy (FT-IR-4100 JASCO, Japan). FT-IR technique is an important technique used in identifying

characteristic surface functional groups on the adsorbent, which in some cases are responsible for the binding of the adsorbate molecules. The spectrum was recorded from 4000 to 400 /cm adopting the KBr pellet method of sample handling.

2.5 Adsorption Experiments

The adsorption experiments of oxamyl onto ASAC were carried out in a set of 150 Erlenmeyer flasks. 100 ml of the pesticide solutions of various initial concentrations in the range 500-2500 mg/L were added to separate flasks and a fixed dose of 2g of the ASAC was added to each flask covered with glass stopper at normal pH (6.7), room temperature ($25^{\circ}\text{C} \pm 2$), for contact time 24h, with occasional agitation to reach equilibrium. The ASAC dose used is the optimum in the range of initial concentrations of pesticide studied and was obtained from preliminary studies.

For kinetic studies of oxamyl onto activated carbon, 100 ml of the solution containing 1000 mg/L with 2g of ASAC for different time intervals from 5 to 360 minutes to determine the equilibrium time at room temperature ($25^{\circ}\text{C} \pm 2$). From the triplicate flasks, 40 ml of filtrate was transferred to a separatory funnel and extracted successively three times with 20, 15 and 10 mL portions of dichloromethane. The combined extract was dried on anhydrous sodium sulfate to remove moisture content and evaporated using a rotary evaporator on a water bath at 40°C . All samples should be cleaned by filtration with Target Nylon ($0.45 \mu\text{m}$) prior to analysis in order to minimize the interference of the carbon fines with the analysis. The extracted samples were analyzed using HPLC with DAD.

Isothermal studies of oxamyl was conducted with an adsorbent quantity of 2g with oxamyl concentration of 500, 1000, 1500, 2000 and 2500 mg/L in identical conical flasks containing 100 ml of distilled water. Blank solutions were treated similarly (without adsorbent).

The sorption capacity was determined by using the following equation, taking into account the concentration difference of the solution at the beginning and at equilibrium [26].

$$q_e = \frac{(C_0 - C_e)V}{m} \quad (1)$$

Where C_0 and C_e are the initial and the equilibrium oxamyl concentration mg/L, respectively, V is the volume of solution (ml) and m is the amount of adsorbent used (g). The percent removal of oxamyl from solution was calculated by the following equation:

$$\text{Removal}(\%) = \frac{(C_0 - C_e)}{C_0} \times 100 \quad (2)$$

2.6. Analysis of Oxamyl

The concentrations of oxamyl in the solutions before and after adsorption were determined using an Agilent HPLC 1260 infinity series (Agilent technologies) equipped with a quaternary pump, a variable wavelength diode array detector (DAD), an auto-sampler with an electric sample valve. The column was Nucleosil C_{18} ($30 \times 4.6 \text{ mm (i.d)} \times 5 \mu\text{m}$) film thickness. The mobile phase was 60/40 (V/V) mixture of HPLC grade acetonitrile /water. The mobile phase flow rate was 1 ml/min. The wavelength was 220 nm. The retention time of oxamyl was 2.4 min and the injection volume was $5 \mu\text{L}$ under the conditions.

3. RESULTS AND DISCUSSION

3.1 Characterization of Activated Carbon

3.1.1 Fourier transform infrared (FTIR) analysis

The FTIR spectrum analysis is important to identify the characteristic functional groups of the biosorbent, which are responsible for adsorption of pesticide molecules. The data in Fig. 1. shows a broad band ranging from 3409-3350/cm represent O-H stretching, two bands at 2807 & 2909/cm correspond to stretching of the C-H bonds of the methyl and methylene groups present in the structure. Band around 2361.41/cm is characteristic of the C=C stretching vibration of alkyne groups [27]. Peak occurring at 1529.27/cm is characteristic of C=C stretching vibration of aromatic ring [28]. The peak observed at 1730.8/cm is due to C=O stretching in the ketone, aldehydes, lactones or carboxyl groups. From the FTIR analysis, it is clear that some surface functional groups are present on the ASAC that might be involved in the pesticide adsorption process.

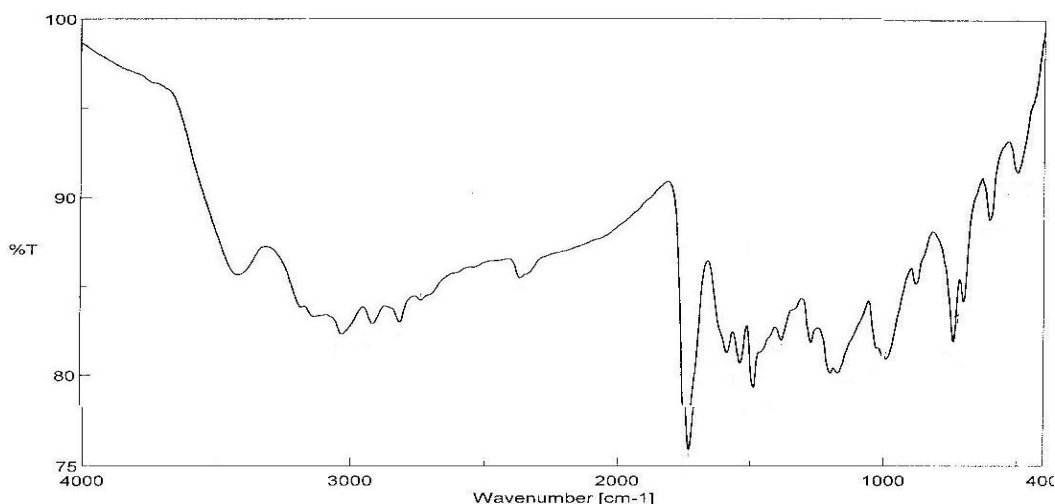


Fig. 1. Fourier transform infrared (FTIR) spectrum of ASAC

3.1.2 Scanning electron microscopy

The microstructure of the ASAC was observed by SEM at 200x magnification and is shown in Fig. 2. This figure shows that the adsorbent had an irregular shape and porous surface, indicating relatively high surface areas. The size distribution of micropores of activated carbon had no definite morphology. This observation is supported by the BET surface area of the ASAC. The values of BET surface areas and average pore diameter obtained for ASAC were 566 m²/g and 0.32 nm, respectively. According to the IUPAC recommendation, total porosity can be classified into three groups which were macropores (d>50 nm), mesopores (2<d<50 nm) and micropores (d<2 nm). Based on the average pore diameter value, ASAC falls into the category of micropores.

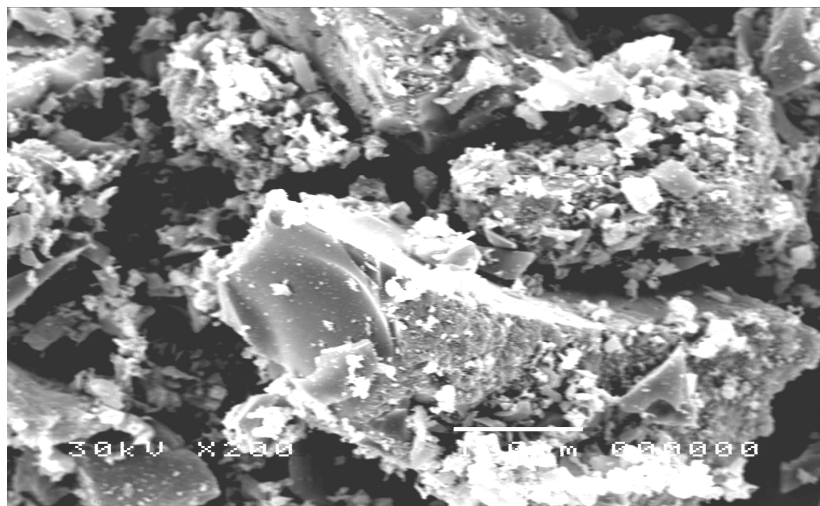


Fig. 2. Scanning electron microscopy (SEM) of ASAC

3.2 Effect of Contact Time and Initial Oxamyl Concentration

In order to determine the equilibrium time for maximum uptake, a contact time study was performed with initial concentrations of oxamyl of 1000 mg/L by ASAC. A graphical representation of the contact time as given in Fig. 3. suggests that the adsorption increased with contact time in 200 min and equilibrium adsorption was established within 240 min. It can be seen that the adsorption of oxamyl is rapid at the initial stage of the contact period, but it gradually slows down until it reaches equilibrium. The fast adsorption at the initial stage may be due to the fact that a large number of surface sites are available for adsorption. As a result, the remaining vacant surface sites are difficult to be occupied due to formation of repulsive forces between the oxamyl molecules on the solid surface and in the bulk phase [29]. Further increase in contact time did not enhance the adsorption, so, the optimum contact time was selected as 240 min for further experiments.

The initial concentration provides an important driving force at overcome all mass transfer resistance of oxamyl between the aqueous and solid phase. The experimental result of the adsorption of oxamyl by ASAC was studied at different initial pesticide concentrations 500, 1000, 1500, 2000 and 2500 mg/L). The wide range of initial concentration of oxamyl was used to observe the adsorption performance of ASAC for oxamyl at both low and high concentrations of oxamyl. The results showed that equilibrium adsorption capacity increased with increase in initial concentration of oxamyl, revealing an increase in equilibrium adsorption capacity from 24.49 to 116.25 mg/g with increasing in the initial pesticide concentration from 500 to 2500 mg/L. The increase in equilibrium adsorption capacity may be due to the utilization of all available active sites for adsorption at higher oxamyl concentration, a larger mass transfer driving force and increased number of collision between pesticide molecules and ASAC. It was also observed that an increase in oxamyl initial concentration resulted to decrease in percent removal (R%) at equilibrium Fig. 4. With an increase in initial concentration of oxamyl from 500 to 2500 mg/L, R% decreased from 97.04 to 92.99%. The decrease in R could be attributed to the saturation of available active sites on ASAC with increase in oxamyl concentration. However, high percent removal was observed even at low initial concentrations of oxamyl.

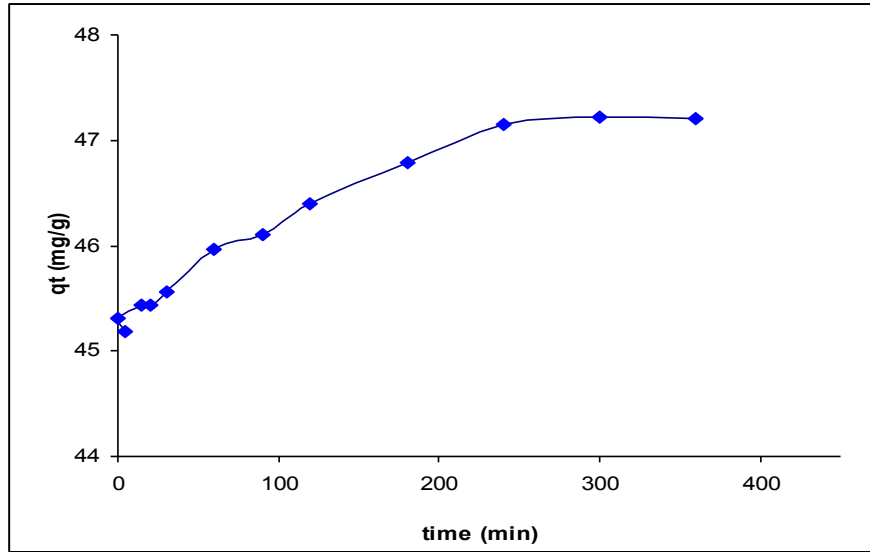


Fig. 3. Effect of contact time for removal of oxamyl by ASAC ($C_0 = 1000 \text{ mg/L}$, pH 6.7, temperature: $25 \pm 2^\circ\text{C}$)

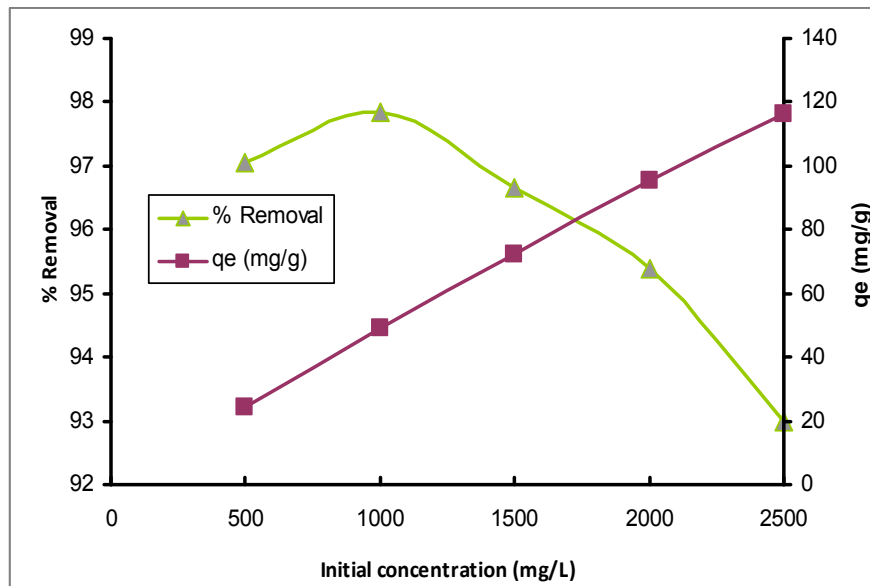


Fig. 4. Effect of initial concentration for removal of oxamyl by ASAC

3.3 Effect of Biosorbent Mass on Oxamyl Adsorption

The adsorbent dose is an important parameter because this parameter determines the capacity of adsorbent for a given pesticide concentration and also determines sorbent-sorbate equilibrium of the system. The effect of adsorbent mass on the adsorption of oxamyl was determined within the adsorbent mass range of (0.1–2.5g/100 ml) in the solution while

keeping the initial oxamyl concentration (2000 mg/L), temperature (25± 2°C) and pH (6.7) constant at contact time for 24h and the results are represented in Fig. 5. The removal efficiency increased from 19 to 96%, as the ASCA dose increased from 0.1g to 2.5g/100 ml. At this dose (2.0g), the removal efficiency was almost constant. This increase in the adsorption with adsorbent dose can be attributed to the increased ASAC surface area and availability of more adsorption sites.

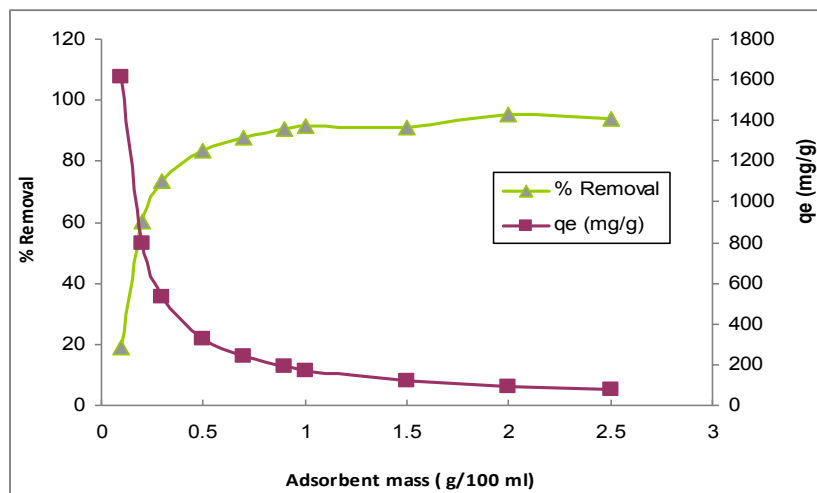


Fig. 5. Effect of adsorbent dose on oxamyl removal onto ASAC (C_0 : 2000 mg/L, pH 6.7, temperature: 25±2°C)

3.4 Biosorption Kinetics

The kinetics of adsorption is an important characteristic to define the efficiency of adsorption. The kinetics of oxamyl adsorption onto ASAC is required for selecting optimum operating conditions for the full-scale batch process. The kinetic parameters, which are helpful for the prediction of adsorption rate give important information for designing and modeling the adsorption processes. Thus, the kinetics of oxamyl adsorption onto ASAC were analyzed using pseudo-first-order [30,31], pseudo-second-order [32] and intraparticle diffusion kinetic models [33]. The conformity between experimental data and the model-predicted values was expressed by the correlation coefficients (R^2 , values close or equal to 1). The relatively higher value is the more applicable model to the kinetics of oxamyl adsorption onto ASAC.

3.4.1 The pseudo first-order

The pseudo first-order rate equation can be expressed in a linear form as:

$$\log(q_e - q_t) = \log(q_e) - \frac{K_1}{2.303}(t) \quad (3)$$

Where q_e and q_t are the amount of oxamyl adsorbed (mg/g) on the adsorbent at the equilibrium and at time t , respectively and k_1 is the rate constant of adsorption (min^{-1}). Values of k_1 were calculated from the plots of $\log(q_e - q_t)$ versus t . The application of this equation to the data of oxamyl on ASAC (data not shown) indicated the inapplicability of the model.

3.4.2 The pseudo-second order

The pseudo-second order kinetic model equation is expressed as:

$$\frac{t}{q_t} = \frac{1}{K_2 q_e^2} + \frac{1}{q_e} t \quad (4)$$

Where k_2 is the rate constant for the pseudo-second order kinetics (g /mg min). The constants can be obtained from plotting (t/q_t) versus t . The initial sorption rate can be calculated using the relation [34].

$$K_0 = K_2 q_e^2 \quad (5)$$

If the second-order kinetics is applicable, then the plot of t/q_t versus t should show a linear relationship. Values of k_2 and equilibrium adsorption capacity q_e were calculated from the intercept and slope of the plots of t/q_t versus t Fig. 6. The linear plots of t/q_t versus t show good agreement between experimental and calculated q_e values Table 2. The correlation coefficients for the second-order kinetic model are greater than 0.999, which led to believe that the pseudo second- order kinetic model provided good correlation for the adsorption of oxamyl onto ASAC. The good correlation coefficients and the calculated values of q_e which are in agreement with experimental values suggest that the adsorption of oxamyl follows the pseudo-second order kinetic model. Ayranci and Hoda (2005) [35] found that the adsorption processes for pesticides Ametryn, Aldicarb, Dinoseb and Diuron from aqueous solution onto high specific surface area activated carbon-cloth followed the pseudo-second order model. Similar results were also reported for the adsorption of 2,4 dichlorophenoxyacetic acid and carbofuran on carbon slurry, blast furnace slag, dust and sludge, 2, 4 dichlorophenol on the surface of maize cob activated carbon [36] and drin on the surface of acid treated olive stones [37].

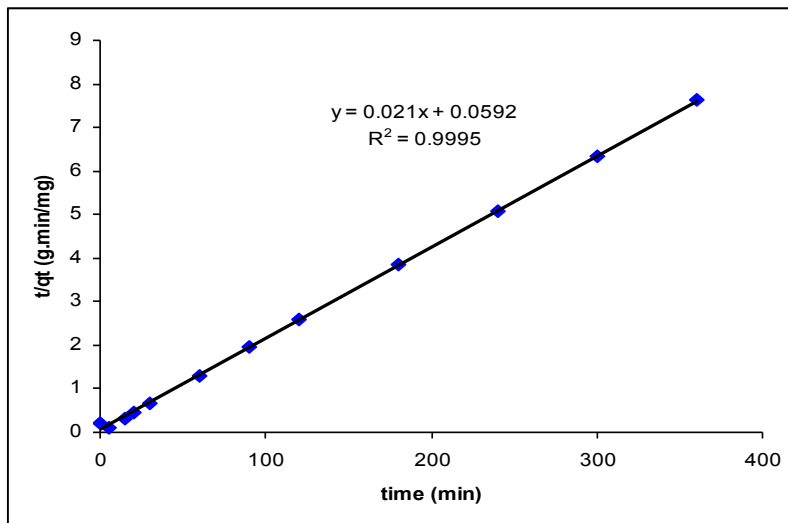


Fig. 6. Pseudo-second-order kinetics for adsorption of oxamyl onto ASAC, $C_0 = 1000$ mg/L, temperature: $25 \pm 2^\circ\text{C}$

3.4.3 The intraparticle diffusion model

The intraparticle diffusion rate was also used for the adsorption of oxamyl on ASAC. The intraparticle diffusion described by Weber and Morriss. The rate constants, for the intraparticle diffusion (K_i) are determined using equation given by Weber and Morriss (1963).

$$q_t = k_i t^{1/2} + C \quad (6)$$

Where K_i is the intraparticle diffusion rate constant ($\text{mg/g min}^{1/2}$) and C (mg/g) is a constant that gives an idea about the thickness of the boundary layer, i.e. the larger the value of C the greater the boundary layer effect. The value of K_i was calculated from the slope of the linear plot of q_t versus $t^{1/2}$. According to this model, if the regressions of q_t versus $t^{1/2}$ is linear and pass through the origin, then intraparticle diffusion is the rate-controlling step. The intraparticle diffusion rate constants values are shown in Table 2. It can be seen from Fig. 7. that the regression was linear but the plot did not pass through the origin, suggesting that adsorption of oxamyl on ASAC involved intraparticle diffusion but not the only rate controlling step. Other kinetic models may control the adsorption rate. Ofomaja (2007) [38] had noted the similar trend for dye adsorption on palm kernel fiber at various initial concentrations. He reported that the multiple nature observed in the intraparticle diffusion plot suggests that intraparticle diffusion is not solely rate controlling. The data for the adsorption of oxamyl on ASAC applied to intraparticle diffusion model as shown in Fig. 7. Three possible mechanisms may occur. The first may be considered as an external surface adsorption or faster adsorption stage. The external surface adsorption (stage1) is absent. The second may describe the gradual adsorption stage, where intraparticle diffusion is rate-controlled. The third one is attributed to the final equilibrium stage, where intraparticle diffusion starts to slow down due to the extremely low adsorbate concentrations in the solution [39,40].

The results demonstrated that the value of coefficient of determination (R^2) for the intraparticle diffusion was slightly lower than those of a pseudo-second order kinetic model indicating that pseudo-second order model is better obeyed than intraparticle diffusion model.

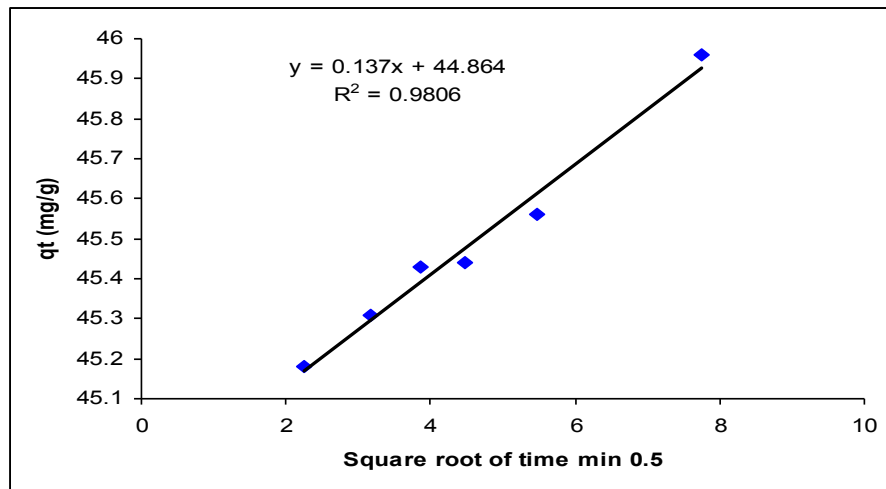


Fig. 7. Intraparticle diffusion for adsorption of oxamyl onto ASAC, $C_0 = 1000 \text{ mg/L}$, temperature: $25 \pm 2^\circ\text{C}$

Table 2. Kinetic constant parameters obtained for oxamyl on ASAC at 25°C

Kinetic model	Parameter	Value
pseudo-second order	K_2 (g/mg. min)	0.0074
	K_0 (g/mg.min)	16.780
	R^2	0.9995
	$q_{e,cal}$ (mg/g)	47.619
Intraparticle diffusion model	k_i (mg/g min ^{1/2})	0.137
	R^2	0.980

3.5 Biosorption Isotherms

Adsorption isotherms are mathematical models that describe the distribution of the adsorbate species between the liquid phase and the solid phase when the adsorption reaches equilibrium state. The adsorption isotherm is important from both a theoretical and a practical point of view. Isotherm data should accurately fit into different isotherm models to find a suitable model that can be used for the design process [41]. The parameters obtained from the different models provide important information on the sorption mechanisms, the surface properties and affinities of the adsorbent. There are several isotherm equations available for analyzing experimental sorption equilibrium data.

The experimental data obtained in the present work was tested with the Langmuir, Freundlich, Temkin, Dubinin-Radushkevich (D–R) and generalized isotherm equations. Linear regression is frequently used to determine the best-fitting isotherm and the applicability of isotherm equations is compared by judging the correlation coefficients.

3.5.1 Langmuir isotherm

The Langmuir equation, which is valid for monolayer adsorption onto a completely homogeneous surface with a finite number of identical sites and with negligible interaction between adsorbed molecules is represented in the linear form as follows Langmuir (1916) [42].

$$\frac{C_e}{q_e} = \frac{1}{Q_m b} + \frac{C_e}{Q_m} \quad (7)$$

Where q_e (mg/g) and C_e (mg/L) are the amount of adsorbed oxamyl per unit mass of adsorbent and oxamyl concentration at equilibrium, respectively. Q_m is the maximum amount of the oxamyl per unit mass of adsorbent to form a complete monolayer on the surface bound at high C_e and b is a constant related to the affinity of the binding sites (L/mg). The plot of specific adsorption (C_e/q_e) against the equilibrium concentration (C_e) (Fig. 8.) shows that the adsorption obeys the Langmuir model. The Langmuir constants Q_m and b were determined from the slope and intercept of the plot and are presented in Table 3.

The essential characteristics of the Langmuir isotherm can be expressed in terms of a dimensionless constant separation factor R_L that is given by Eq. (8) [43].

$$R_L = \frac{1}{1 + K_L C_0} \quad (8)$$

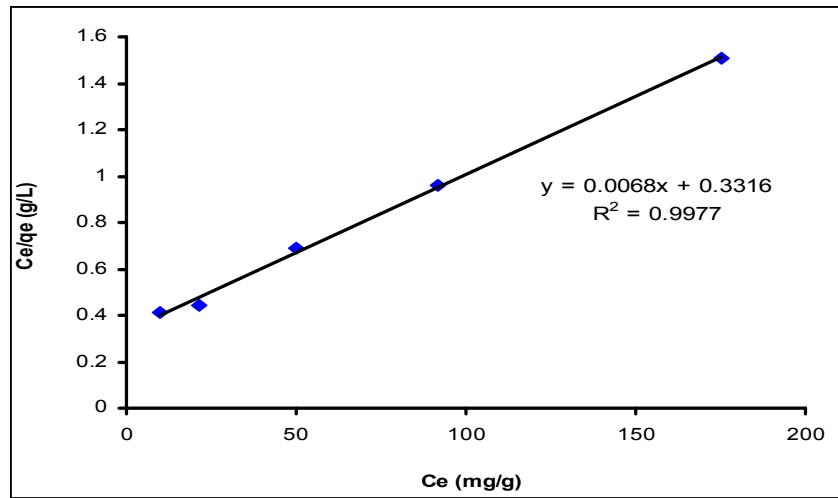


Fig. 8. Langmuir adsorption isotherm of oxamyl on ASAC

Where C_0 is the highest initial concentration of adsorbate (mg/L) and K_L (L/mg) is Langmuir constant. The R_L values between 0 and 1 indicate favorable adsorption. R_L values indicate the type of isotherm to be irreversible ($R_L=0$), favourable ($0 < R_L < 1$), linear ($R_L=1$) or unfavourable ($R_L > 1$). The value of R_L in the present investigation was found to be 0.00039 indicating that the adsorption of oxamyl on ASAC is favorable.

Table 3. Langmuir, Freundlich, Temkin and Dubinin–Radushkevich (D-R) isotherm models constants and correlation coefficients for adsorption of oxamyl on prepared activated carbon

Parameters	Isotherm model
147.05	Langmuir isotherm
0.020	q_m (mg/g)
0.9977	K_L (L/mg)
	R^2
8.28	Freundlich isotherm
0.5323	K_F
0.960	$1/n$
	R^2
128.4	Temkin isotherm
37.924	A (L/g)
0.9551	B
	R^2
121.75	D-R isotherm
2.611×10^{-8}	q_m (mg/g)
4.37	β (mol ² /J ²)
0.9948	E (KJ/mol)
	R^2

The Langmuir isotherm fits quite well with the experimental data (correlation coefficient $R^2 > 0.99$). The monolayer adsorption capacity according to this model was 147.05 mg/g. The fact that the Langmuir isotherm fits the experimental data very well may be due to homogeneous distribution of active sites onto ASAC surface, since the Langmuir equation

assumes that the surface is homogenous. A similar result was reported in literature for the adsorption of parquet dichloride from aqueous solution by activated carbon derived from used tires Hamadi et al. (2004) [43].

3.5.2 The freundlich isotherm

The Freundlich isotherm is an empirical equation which is used to describe on heterogeneous surface and active sites with different energy Freundlich (1906) [44]. The Freundlich isotherm can be derived assuming a logarithmic decrease in the enthalpy of sorption with the increase in the fraction of occupied sites and is commonly given by the following non-linear equation:

$$q_e = K_f C_e^{\frac{1}{n}} \quad (9)$$

Where q_e (mg/g) is the equilibrium value for removal of adsorbate per unit weight of adsorbent, C_e (mg/L) is the equilibrium concentration of pesticide in solution, and K_f is the Freundlich constant (mg/g)(L/mg)^{1/n} related to the bonding energy. K_f can be defined as the adsorption or distribution coefficient and represents the quantity of pesticide adsorbed onto adsorbent for unit equilibrium concentration. $1/n_f$ is the heterogeneity factor and n_f is a measure of the deviation from linearity of adsorption.

Eq. (9) can be linearized in the logarithmic form (Eq. (10)) and the Freundlich constants can be determined:

$$\log q_e = \log K_f + 1/n \log C_e \quad (10)$$

The applicability of the Freundlich sorption isotherm was also analyzed, using the same set of experimental data, by plotting $\log (q_e)$ versus $\log (C_e)$. The data obtained from linear Freundlich isotherm plot for the adsorption of the oxamyl onto ASAC is presented in Fig.9. and Table 3. The $1/n$ is lower than 1.0, indicating that oxamyl is favorably adsorbed by ASAC.

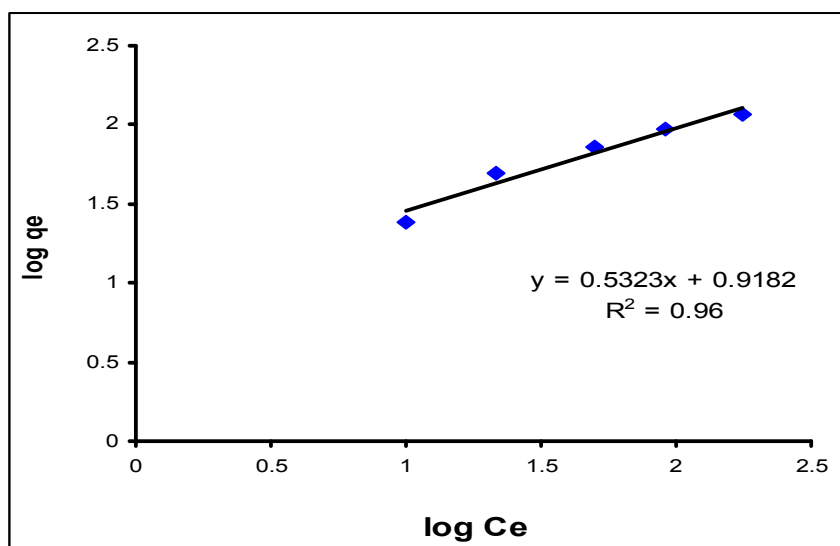


Fig. 9. Freundlich adsorption isotherm for oxamyl adsorption on ASAC.

3.5.3. The Temkin isotherm

Temkin adsorption isotherm model was used to evaluate the adsorption potentials of the ASAC for oxamyl. The derivation of the Temkin isotherm assumes that the fall in the heat of sorption is linear rather than logarithmic, as implied in the Freundlich equation. The Temkin isotherm has commonly been applied in the following form [45].

$$q_e = \frac{RT}{b} \ln(AC_e) \quad (11)$$

The Temkin isotherm, Eq. (11) can be simplified to the following equation:

$$q_e = \beta \ln \alpha + \beta \ln C_e \quad (12)$$

Where $\beta=(RT)/b$, T is the absolute temperature in Kelvin and R is the universal gas constant, 8.314 J (mol /K). The constant b is related to the heat of adsorption. q_e (mg/g) and C_e (mg/L) are the amount adsorbed at equilibrium and the equilibrium concentration, respectively. A and B are constants related to adsorption capacity and intensity of adsorption. Plots of $\ln C_e$ against q_e for the adsorption of oxamyl onto ASAC are given in Fig.10. The constants A and B are listed in Table 3.

Examination of the data shows that the Temkin isotherm is not applicable to oxamyl adsorption onto ASAC judged by low correlation coefficient $R^2=0.9551$.

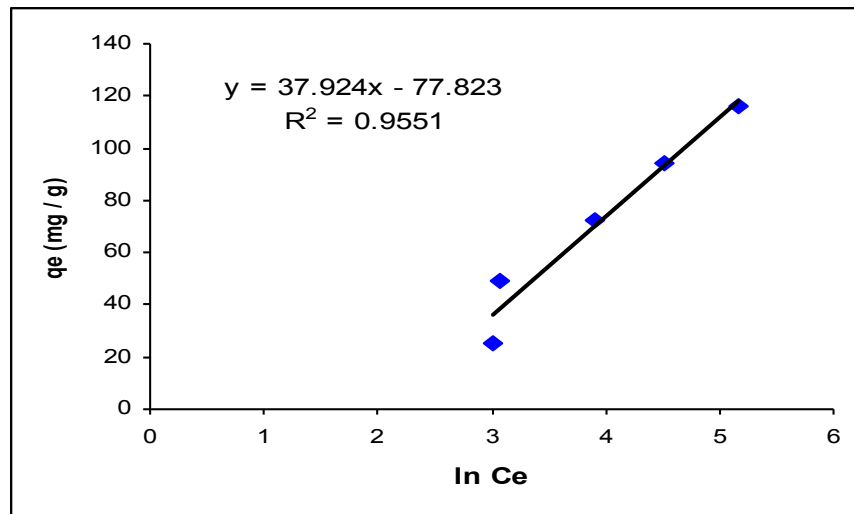


Fig. 10. Temkin adsorption isotherm for oxamyl adsorption on ASAC.

3.5.4 The dubinin–radushkevich (D–R) isotherm

Another equation used in the analysis of isotherms was proposed by Dubinin-Radushkevich. D–R model was applied to estimate the porosity apparent free energy and the characteristic of adsorption Dubinin (1965) [46]. The D–R isotherm does not assume a homogeneous surface or constant sorption potential and it has commonly been applied in the following form (Eq. (13)) and its linear form can be shown in Eq. (14):

$$q_e = q_m \exp(-K\varepsilon^2) \tag{13}$$

$$\ln q_e = \ln q_m - \beta \varepsilon^2 \tag{14}$$

Where K is a constant related to the adsorption energy, q_e (mg/g) is the amount of pesticide adsorbed per g of adsorbent and q_m represents the maximum adsorption capacity of adsorbent, β (mol^2/J^2) is a constant related to adsorption energy, while ε is the Polanyi potential can be calculated from Eq. (15):

$$\varepsilon = RT \ln \left[1 + \frac{1}{C_e} \right] \tag{15}$$

The values of β and q_m can be obtained by plotting $\ln q_e$ vs. ε^2 . The mean free energy of adsorption (E, J/mol), defined as the free energy change when one mole of ion is transferred from infinity in solution to the surface of the sorbent, was calculated from the K value using the following relation Eq. (16) Radushkevich (1949) [47].

$$E = \frac{1}{\sqrt{2\beta}} \tag{16}$$

The calculated value of D–R parameters is given in Fig. 11 and Table 3. The saturation adsorption capacity q_m obtained using D–R isotherm model for adsorption of oxamyl onto ASAC is 121.75mg/g. The values of E calculated using Eq. (15) is 4.37 kJ /mol, which indicating that the physico-sorption process plays the significant role in the adsorption of oxamyl onto ASAC.

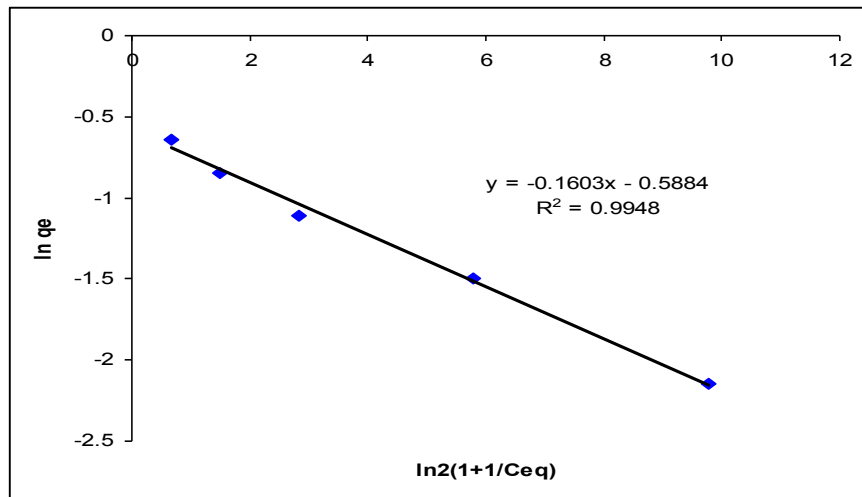


Fig. 11. Dubinin–Radushkevich for oxamyl adsorption on ASAC.

3.6 Biosorption Thermodynamics

Temperature dependence of the adsorption process is associated with several thermodynamic parameters. Thermodynamic considerations of an adsorption process are necessary to conclude whether the process is spontaneous or not. The Gibbs free energy change is an important criterion for spontaneity. Both energy and entropy factors must be considered in order to determine the Gibbs free energy of the process. Thermodynamic parameters such as Gibbs free energy change (ΔG°), enthalpy change (ΔH°) and the entropy change (ΔS°) can be estimated using equilibrium constants changing with temperature. The

Gibbs free energy change of the adsorption reaction can be determined from the following equation:

$$\Delta G^\circ = -RT \ln K_e \quad (17)$$

The K_e value was calculated using the following equation:

$$K_e = \frac{q_e}{C_e} \quad (18)$$

Relation between ΔG , ΔH and ΔS can be expressed by the following equations:

$$\Delta G^\circ = \Delta H^\circ - T\Delta S^\circ \quad (19)$$

Eq. (19) can be written as:

$$\ln K_e = -\frac{\Delta G^\circ}{RT} = -\frac{\Delta H^\circ}{RT} + \frac{\Delta S^\circ}{R} \quad (20)$$

According to the Eq. (20), ΔH and ΔS parameters can be calculated from the slope and intercept of the plot of $\ln K_e$ versus $1/T$, respectively [48]. The thermodynamic parameters calculated according to Eqs. (17) and (20) are listed in Table 4. and Fig. 12. The ΔG° is negative and changes with the rise in temperature, which suggests that the adsorption process is spontaneous in the nature and the spontaneity increases with the rise in temperature. The enthalpy change (6.42 KJ/mol) of the system is positive and smaller than 40 KJ/mol, indicating that the adsorption of oxamyl onto ASAC is endothermic and physical in nature [49]. The positive value of ΔS° implies increased randomness at the solid-solution interface with some structural changes during adsorption process.

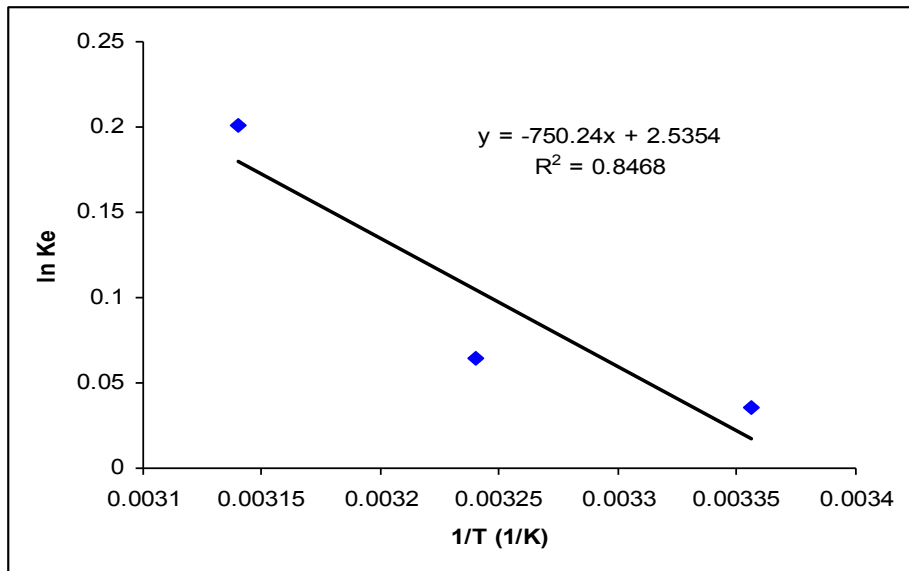


Fig. 12. Plot of $\ln K_e$ against $1/T$ for adsorption of oxamyl onto ASAC.

Table 4. Thermodynamic parameters for the adsorption of oxamyl on ASAC

$-\Delta G^\circ$ (KJ/mol)			ΔH° (KJ/mol)	ΔS° (J/mol K)
298 K	308 K	318 K	6.42	21.657
6.44	6.66	6.88		

4. CONCLUSION

The present investigation showed that waste of apricot stones can be effectively used as a raw material for the preparation of activated carbon for removal of oxamyl from aqueous solutions. The adsorption of oxamyl on activated carbon is found to be initial concentration, adsorbent dose and contact time dependent. The adsorption equilibrium was achieved after 240 min. The equilibrium data fitted well with the Langmuir isotherm. The monolayer adsorption capacity was found as 147.05 mg/g.

The kinetic study of the adsorption of oxamyl shows that the pseudo-second order model provides better correlation of the adsorption data. The intraparticle diffusion was not the rate-controlling step. Thermodynamic parameters suggested that the adsorption of oxamyl on apricot stone activated carbon was feasible, spontaneous and endothermic in nature.

These results show that ASAC which have a very low economical value may be used effectively for removal of oxamyl from aqueous solution for environmental protection purpose.

COMPETING INTERESTS

Authors have declared that no competing interests exist.

REFERENCES

1. Mowry TM. Insecticidal reduction of potato leafroll virus transmission by *Muzus persicae*. *Annals of Applied Biology*. 2005;146:81–88.
2. Tomlin CDS. *The e-Pesticide Manual*, Version 2.2. The British Crop Protection Council, Surrey, UK; 2002.
3. Minnis ST, Haydock PPJ, Evans K. Control of potato cyst nematodes and economic benefits of application of 1,3-dichloropropane and granular nematicides. *Annals of Applied Biology*. 2004;145:145–156.
4. Philip HH, Michalenko EM, Jarvis WF, Basu DK, Sage GW, Meyland WM, Beauman JA. Gray (Eds.), *Handbook of Environmental Fate and Exposure Data for Organic Chemicals*, vol. III, Lewis, Chelsea, MI; 1991.
5. Uğurlu M, Karaoğlu MH. TiO_2 supported on sepiolite : preparation, structural and thermal characterization and catalytic behaviour in photocatalytic treatment of phenol and lignin from olive mill wastewater, *Chem. Eng. J.* 2011;166:859–867.
6. Gong J, Yang C, Zhang W, Pu J. Liquid phase deposition of tungsten doped TiO_2 films for visible light photoelectrocatalytic degradation of dodecyl benzenesulfonate, *Chem. Eng. J.* 2011;167:190–197.
7. Katsumata H, Kobayashi T, Kaneco S, Suzuki T, Ohta K. Degradation of linuron by ultrasound combined with photo-Fenton treatment, *Chem. Eng. J.* 2011;166:468–473.

8. Zhou T, Lim TT, Chin SS, Fane AG. Treatment of organics in reverse osmosis concentrate from a municipal wastewater reclamation plant: feasibility test of advanced oxidation processes with/without pretreatment, *Chem. Eng. J.* 2011;166:932–939.
9. Rajashekara Murthy HM, Manonmani HK. Aerobic degradation of technical hexachlorocyclohexane by a defined microbial consortium, *J. Hazard Mater.* 2007;149:18–25.
10. Banasiak LJ, Van der Bruggen B, Schäfer AI. Sorption of pesticide endosulfan by electro dialysis membranes, *Chem. Eng. J.* 2011;166:233–239.
11. Maldonado MI, Malato S, Perez-Estrada LA, Gernjak W, Oller I, Domenech X, Peral J. Partial degradation of five pesticides and an industrial pollutant by ozonation in a pilot-plant scale reactor, *J. Hazard Mater.* 2006;38:363–369.
12. Al-Muhtase AH, Ibrahim KA, Albadarin AB, Ali-khashman O, Walker GM, Ahmad MNM. Remediation of phenol-contaminated water by adsorption using poly (methyl methacrylate) (PMMA), *Chem. Eng. J.* 2011;168:691–699.
13. Hameed BH, Ahmad AL, Latiff KNA. Adsorption of basic dye (methylene blue) onto activated carbon prepared from rattan sawdust, *Dyes Pigments.* 2007;75:143–149.
14. Tan IAW, Hameed BH, Ahmad AL. Equilibrium and kinetic studies on basic dye adsorption by oil palm fibre activated carbon, *Chem. Eng. J.* 2007;127:111–119.
15. Hameed BH, Din ATM, Ahmad AL. Adsorption of methylene blue onto bamboo-based activated carbon: kinetics and equilibrium studies, *J. Hazard Mater.* 2007;141:819–825.
16. Tan IAW, Ahmad AL, Hameed BH. Adsorption of basic dye using activated carbon prepared from oil palm shell: batch and fixed bed studies, *Desalination.* 2008;225:13–28.
17. Maryam K, Mehdi A, Shabnam T, Majdeh M, Hamed R.K. *Journal of Hazardous Materials.* 2008;150:322–327.
18. Dolas H, Sahin O, Saka C, Demir H. A new method on producing high surface area activated carbon: the effect of salt on the surface area and the pore size distribution of activated carbon prepared from pistachio shell, *Chem. Eng. J.* 2011;166:191–197.
19. Ahmad MA, Alrozi R. Optimization of rambutan peel based activated carbon preparation conditions for Remazol Brilliant Blue R removal, *Chem. Eng. J.* 2011a;166:280–285.
20. Ahmad MA, Alrozi R. Optimization of preparation conditions for mangosteen peel-based activated carbons for the removal of Remazol Brilliant Blue R using response surface methodology, *Chem. Eng. J.* 2010 b;165:883–890.
21. Sun Y, Webley PA. Preparation of activated carbons from corncob with large specific surface area by a variety of chemical activators and their application in gas storage, *Chem. Eng. J.* 2010;162:883–892.
22. Yang J, Qiu K. Preparation of activated carbons from walnut shells via vacuum chemical activation and their application for methylene blue removal, *Chem. Eng. J.* 2010;165:209–217.
23. Anonymous, *Agricultural Statistics, Economic Affairs Sector, Egyptian Ministry of Agriculture and land Reclamation, Cairo (2005).*
24. Tomlin CDS. *The e-Pesticides Manual, version 3.0, 13th ed., BCPC (British Crop Protection Council), Copyright ©; 2004.*
25. Njoku VO, Hameed BH. Preparation and characterization of activated carbon from corncob by chemical activation with H_3PO_4 for 2,4-dichlorophenoxyacetic acid adsorption, *Chem. Eng. J.* 2011;173:391-399.
26. Arslanoglu FN, Kar F, Arslan N. Adsorption of dark coloured compounds from peach pulp by using powdered activated carbon, *J. Food Eng.* 2005;71:156–163.

27. Smith B. *Infrared Spectral Interpretation: A Systematic Approach*, CRC Press, Boca Raton; 1999.
28. Ren L, Zhang J, Li Y, Zhang C. Preparation and evaluation of cattail fiber-based activated carbon for 2,4-dichlorophenol and 2,4,6-trichlorophenol removal, *Chem. Eng. J.* 2011;168:553–561.
29. Mohd Din AT, Hameed BH, Ahmad AL. Batch adsorption of phenol onto physiochemical-activated coconut shell. *J. Hazard Mater.* 2009;161:1522–1529.
30. Lagergren S. Zurtheorie der sogenannten adsorption gelöster stoffe, *Kungliga Svenska Vetenskapsakademiens Handlingar.* 1898;24:1–39.
31. Febrianto J, Kosasih AN, Sunarso J, Ju YH, Indraswati N, Ismadji S. Equilibrium and kinetic studies in adsorption of heavy metals using biosorbent: a summary of recent studies, *J. Hazard. Mater.* 2009;162:616–645.
32. Ho YS, McKay G, Wase DAJ, Foster CF. Study of the sorption of divalent metal ions on the peat, *Adsorp. Sci. Technol.* 2000;18:639–650.
33. Weber WJ, Morriss JC. Kinetics of adsorption on carbon from solution, *J. Sanit. Eng. Div. Am. Soc. Civil Eng.* 1963;89:31–60.
34. Koynucu H. Adsorption Kinetics of 3- hydroxybenzaldehyde on native and activated bentonite, *Appl. Clay Sci.* 2008;38:279.
35. Ayranci E, Hoda N. Adsorption kinetics and isotherms of pesticides onto activated carbon-cloth, *Chemosphere* 2005;60:1600–1607.
36. Sathishkumar M, Binupriya AR, Kavitha D, Selvakumar R, Jayabalan R, Choi JG, Yun SE. Adsorption potential of maize cob carbon for 2,4-dichlorophenol removal from aqueous solutions: equilibrium, kinetics and thermodynamics modeling, *Chem. Eng. J.* 2009;147:265–271.
37. El Bakouri H, Usero J, Morillo J, Ouassini A. Adsorptive features of acid-treated olive stones for drin pesticides: equilibrium, kinetic and thermodynamic modeling studies, *Bioresour Technol.* 2009;100:4147–4155.
38. Ofomaja A.E. Kinetics and mechanism of methylene blue sorption onto palm kernel fibre, *Process Biochem.* 2007;42:16–24.
39. Crini C, Peindy HN, Gimbert F, Robert C. Removal of C.I. Basic green 4 (Malachite Green) from aqueous solutions by adsorption using cyclodextrin-based adsorbent—kinetic and equilibrium studies, *Sep. Purif. Technol.* 2007;53:97.
40. Ozacan M. Contact time optimization of two-stage batch adsorber design using second-order kinetic model for the adsorption of phosphate onto alunite, *J. Hazard. B. Mater.* 2006;137:218.
41. Alley ER. *Water Quality Control Handbook*, McGraw-Hill Education Publishers. 2000;125–141. ISBN0070014132/9780070014138/0-07-001413-2 Available: <http://www.bookfinder.com/author/e-roberts-alley/>.
42. Langmuir I. The constitution and fundamental properties of solids and liquids, *J. Am. Chem. Soc.* 1916;38:2221–2295.
43. Hall KR, Eagleton LC, Acrivos A, Vermeulen T. Pore and solid-diffusion kinetics in fixed-bed adsorption under constant-pattern conditions, *I&EC Fundam.* 1966;5:212–223.
44. Freundlich H. -ber die adsorption in lösungen (Adsorption in solution), *Z. Phys. Chem.* 1906;57:384–470.
45. Aharoni C, Sparks DL. Kinetics of soil chemical reactions—a theoretical treatment, in: D.L. Sparks, D.L. Suarez (Eds.), *Rate of Soil Chemical Processes*, Soil Science Society of America, Madison, WI. 1991;1–18.
46. Dubinin MM, Modern state of the theory of volume filling of micropore adsorbents during adsorption of gases and steams on carbon adsorbents, *Zh. Fiz. Khim.* 1965;39:1305–1317.

47. Radushkevich LV. Potential theory of sorption and structure of carbons, *Zh. Fiz. Khim.* 1949;23:1410–1420.
48. Hassa SM, Awwad N, Aboterika AA. Removal of synthetic reactive dyes from textile wastewater by Sorels cement, *J. Hazard Mater.* 2009;162:994-999.
49. Li Y, Yue QY, Gao BY, Li Q, Li CL. Adsorption thermodynamic and kinetic studies of dissolved chromium onto humic acids, *Colloids Surf. B.* 2008;65:25-29.

© 2014 Ahmed et al.; This is an Open Access article distributed under the terms of the Creative Commons Attribution License (<http://creativecommons.org/licenses/by/3.0>), which permits unrestricted use, distribution, and reproduction in any medium, provided the original work is properly cited.

Peer-review history:

The peer review history for this paper can be accessed here:
<http://www.sciencedomain.org/review-history.php?iid=356&id=2&aid=2721>